実際はAMPKはこれまでに図2のような各種作用を有することが知られている．正常細胞では環境に応じてapoptosis, autophagy, cell growthの調整をしている．

糖尿病治療薬メトホルミンはAMPKを活性化する作用を有している[1]．

メトホルミンは糖尿病治療薬としてだけではなく2つの大規模な疫学的研究によって発癌抑制としての可能性も注目されている．一つは英国のケースコントロールスタディで，2型糖尿病患者でメトホルミンの内服の有無による癌の発生について検証したものである[2]．11,876人の新規の2型糖尿病患者が登録され，観察期間内(1993～2001年)に923人が新たに悪性新生物と診断された．メトホルミンの内服は発癌リスクの減少と関連があり，さらに長い期間メトホルミンを内服しているほうが発癌のリスクが低い傾向にあった(図3)．

もう一つはカナダの観察研究で，新規の糖尿病患者でメトホルミンか，スルホニル尿素薬の単独療法の患者を平均5.4年追跡した[3]．計10,309人が対象となり，うち6,969人がメトホルミン，3,340人がスルホニル尿素薬の内服治療であった．結果，癌による死亡率は，メトホルミン群はスルホニル尿素薬群の約2/3であり，メトホルミンに対するスルホニル尿素薬の年齢性別の調整ハザード比は1.3(95% CI 1.1～1.6, P=0.012)であった．

以上のようにこれらのデータはメトホルミンの化学発癌予防薬としての可能性を示しており，実際，これまでに乳癌や前立腺癌，大腸癌などで癌の化学予防薬として積極的に研究がなされている．本稿では，われわれがこれまで行ってきたAMPKを分子標的とした大腸癌化学予防の研究を紹介する．

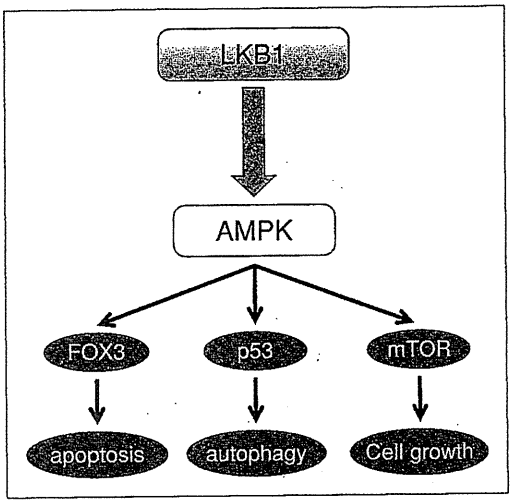

図2　AMPKの細胞増殖，アポトーシス，オートファジーに対する作用

マウス発癌モデルでの検討[4]

1．大腸前癌病変aberrant crypt foci(ACF)形成への影響

メトホルミンによる大腸発癌の予防効果を検討するため，大腸発癌の前癌病変であるACFを指標に検討した．ACF数は普通食群で7.0±0.5個(1匹あたり平均数)であったが，メトホルミン投与群は2.2±0.3個で有意に抑制されていた(P<0.05)(表1)．

2．大腸ポリープ形成への影響

メトホルミン投与群は，普通食群と比べてポリープの数，大きさともに有意に抑制された(表2)．

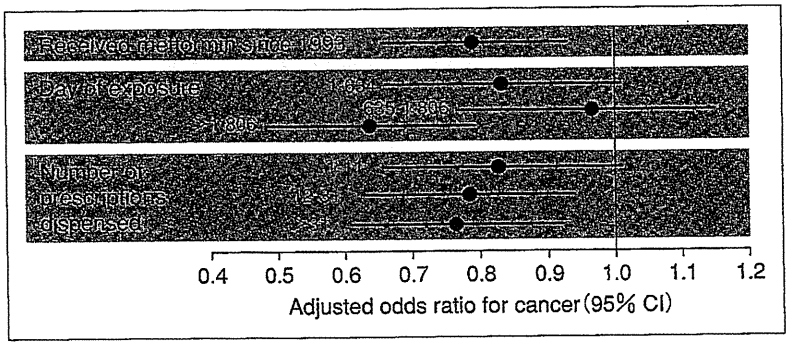

図3　メトホルミン使用患者と非使用者の発癌オッズ比

表1　メトホルミンによるACF抑制効果

食餌	マウス(n)	ACF数(1匹あたり)
普通食(Group1)	12	7.0～0.5
メトホルミン(Group2)	12	2.2～0.3*

*$P<0.05$, 普通食摂取マウスと比較．平均値±SE.

表2　メトホルミンによるポリープ抑制効果

食餌	マウス(n)	ポリープ数	ポリープの大きさ(mm)
普通食	12	8.0～0.4	2.18～0.05
メトホルミン	12	6.4～0.4*	1.19～0.04*

*$P<0.05$, 普通食摂取マウスと比較．平均値±SE.

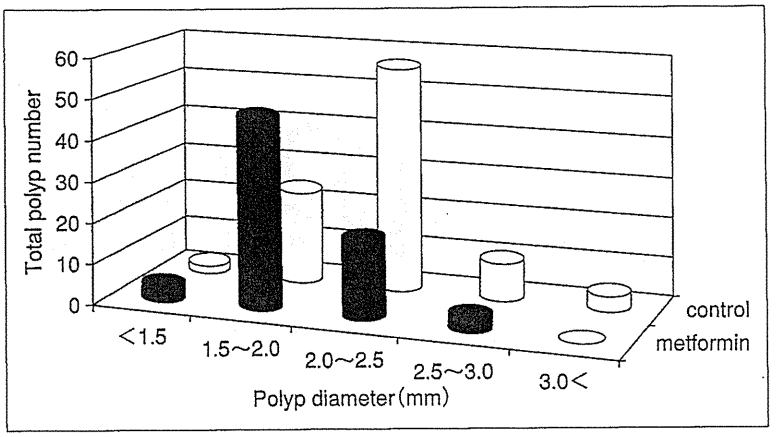

図4　ポリープのサイズ別分布

特に3 mm以上の大きなポリープは，メトホルミン投与群では発生しなかった(図4)．

3．大腸上皮細胞増殖の比較

メトホルミンによるACF形成抑制効果の機序を解明するため，大腸上皮の増殖能をBrdU, PCNA labeling indexで測定した．その結果，普通食群と比較してメトホルミン投与群は両方のindexが低下していた(図5)．これらの結果は，メトホルミンによるACF抑制は，細胞増殖の抑制と関連していることが示唆される．

4．メトホルミン投与によるアポトーシスへの影響

メトホルミン投与がアポトーシスへ影響するかどうかTUNEL法を用いて検討した．図6のようにアポトーシスindexは2群間で有意差はなく，メトホルミンは大腸上皮細胞のアポトーシスには影響がないことが示唆された．

5．メトホルミンによるAMPKの活性化とmTOR経路の抑制

メトホルミン投与で大腸上皮細胞の増殖活性が抑制されている機序を明らかにするため，大腸粘膜の蛋白発現を検証した．メトホルミンの薬理作用のターゲットの一つはAMPKの活性化であり[5]，活性化されたAMPKは下流のmTOR/S6K経路を抑制することが報告されている[6]．そこで大腸上皮においてAMPKとその下流のmTOR, S6K, S6Pの発現についてウエスタンブロット解析を行った．結果，図7-Aのように AMPKのリン酸化の亢進(図7-C)とmTOR, S6K, S6P経路のリン酸化抑制(図7-D～F)が確認できた．さらに，メトホルミンのmTOR経路の抑制はAMPKを介していることを確証するため，Aktのリン酸化がメトホルミン投与で亢進されていないかどうか調べた．ウエスタンブロット解析ではAktのリン酸化は亢進していないことが確認できた(図7-B)．

ヒトでのメトホルミンを用いた大腸癌化学予防の検討

1．メトホルミンが大腸に作用するか？

最近フランスからの報告でメトホルミンを内服すると，糖の取り込みをみるFDG-PETでは主に腸に糖の取り込み増加が顕著に認められた[7]ことから，われわれはヒトに対してメトホルミンは癌の化学予防では大腸癌に非常に有効でないかとの仮説を立て，非糖尿病患者に対してメト

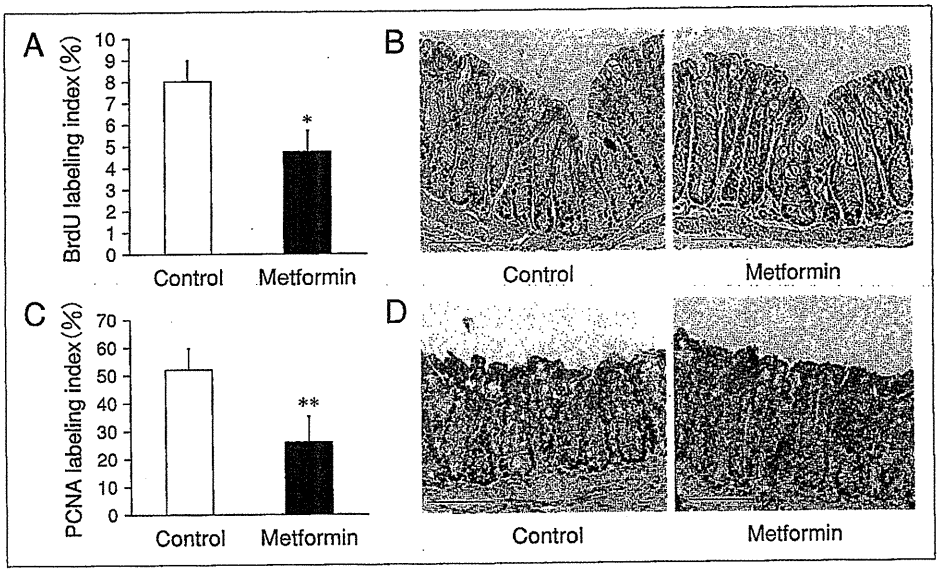

図5　メトホルミン投与による大腸上皮細胞増殖の抑制
A：普通食群とメトホルミン投与群の平均BrdU labeling index．*P<0.05, **P<0.01．Indexは，大腸陰窩における核総数に対する染色陽性細胞の割合で表されている．
B：BrdU免疫組織化学染色像．スケールバー：100μm.
C：普通食群とメトホルミン投与群の平均PCNA labeling index．*P<0.05, **P<0.01．Indexは，大腸陰窩における核総数に対する染色陽性細胞の割合で表されている．
D：PCNA免疫組織化学染色像．スケールバー：100μm.

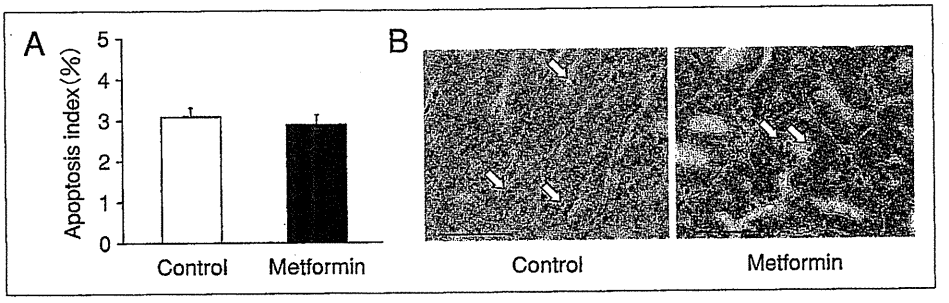

図6　TUNEL法によるアポトーシス解析
A：普通食群とメトホルミン投与群の平均アポトーシスindex．2群間で有意差はなかった．
B：TUNEL染色．矢印はTUNEL陽性シグナル．スケールバー：100μm.

ホルミンを投与して大腸前癌マーカーACFの変化を検討した．

2．試験のデザインと対象症例

2008年5月から2010年5月までの期間に横浜市立大学附属病院で，下部消化管内視鏡検査を施行された重篤な合併症を併発していない非糖尿病患者を対象とした．

下部消化管内視鏡検査時に拡大内視鏡を用いてACFを観察した．症例はメトホルミン投与群とコントロール(無投与)群に無作為に分けられ，メトホルミン投与群はメルビン®1錠/日(メトホルミン250mg含量)の内服を開始した．両群ともに1か月後に下部消化管内視鏡検査を再検し，ACFの数を比較検討した[8]．

対象期間内に26人の非糖尿病患者がエントリーされた．うち12人がメトホルミン群，14人がコントロール群に分けられた．臨床試験開始後，メトホルミン群のうち1人はメトホルミンの内服を途中で中断され，また，2人はフォローのための1か月後の下部消化管内視鏡検査の施行を

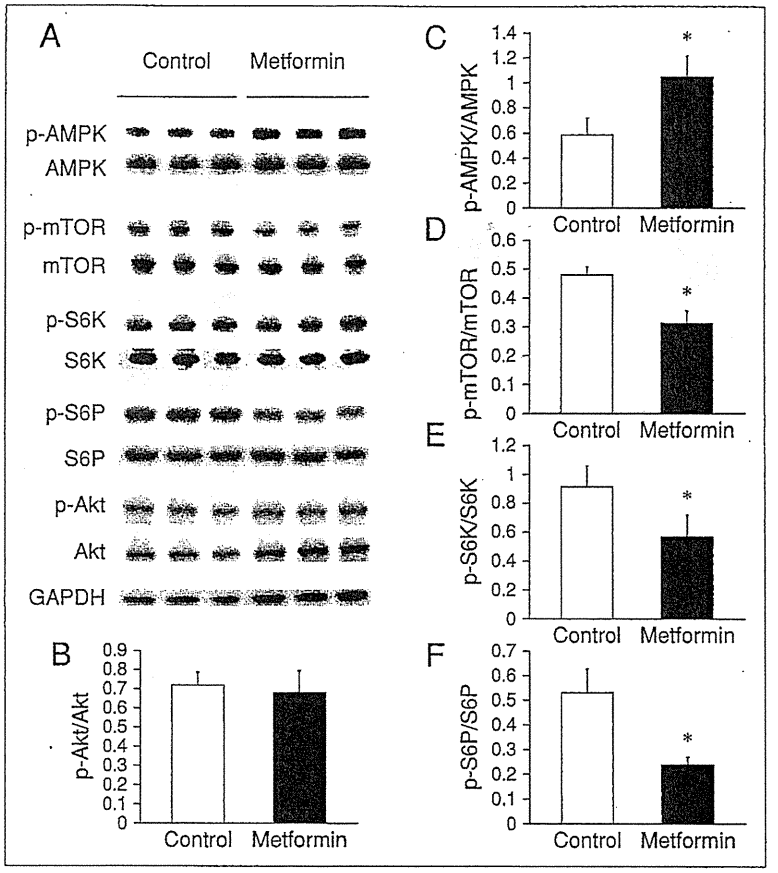

図7 メトホルミン投与によるAMPK経路の比較

A：典型的なウエスタンブロット画像．普通食とメトホルミン投与群のマウスの大腸組織を用いたAPMK, mTOR, S6K, S6P, Aktとそれぞれのリン酸化抗体のウエスタンブロット解析．

B～F：総蛋白レベルに対するリン酸化蛋白の割合のグラフ．平均値±SEで表示．
* $P<0.05$.

表3 患者背景

	P値	メトホルミン群	コントロール群	
患者数		9	14	NS
男性：女性		8：1	12：2	NS
年齢		69.1～5.95	64.2～9.07	NS
BMI(kg/m²)		23.1～3.21	24.3～3.74	NS
HbA1c(%)		5.8～1.01	5.4～0.56	NS
腺腫(数，保有率%)		4(44.4)	6(42.8)	NS
ACF数(1人あたりの平均数)		8.78～6.45	7.23～6.65	NS

NS：non-significant．平均値－SD．

同意されなかった．最終的にメトホルミン群は9人の症例が評価の対象となった．患者背景を表3に示す．患者背景に2群間で有意差はなかった．

3．メトホルミンのACF抑制効果

メトホルミン群において平均ACF数は8.75±6.45個から，1か月後5.11±4.99個に有意に減少した($P=0.007$)．一方，コントロール群は7.23±

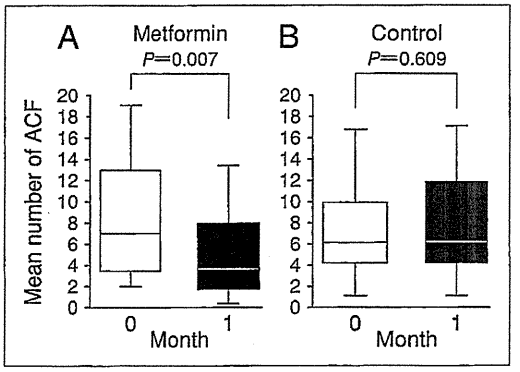

図8　メトホルミンによるACF数の変化
A：メトホルミン群では，ACF数は1か月後有意に減少した．
B：コントロール群ではACF数の有意な変化は認めなかった．
データは箱髭図で表され，長方形の上辺は第3四分位数，下辺は第1四分位数を示し，中央の線は中央値である．

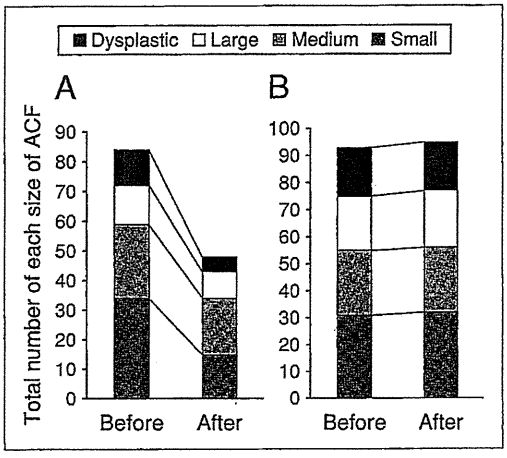

図9　ACFの分布の変化
A：メトホルミン群．1か月間のメトホルミン投与でdysplastic ACFとsmall ACFが半減．
B：コントロール群．1か月間でACFの分布の変化は認めない．

表4　メトホルミン群における血液データ，ACF数の変化

	P値	前	後	
血糖値(mg/dl)		104.8～14.5	101.3～13.4	NS
HbA1c(%)		5.8～1.01	5.7～0.82	NS
HOMA-IR		1.21～1.13	1.20～0.586	NS
総コレステロール(mg/dl)		179.2～63.8	179.0～66.2	NS
中性脂肪(mg/dl)		112.5～29.8	107.0～41.2	NS
ACF数(平均値)		8.78～6.45	5.11～4.99	0.007

NS：non-significant．平均値－SD．

6.65個から，1か月後7.56±6.75個と有意な変化はなかった(P= 0.609)(図8)．ACFのサイズやdysplastic ACFの分布変化については図9のとおりで，メトホルミン群ではdysplastic ACFとsmall ACFが半減したが，コントロール群では変化はなかった．

本研究においては，1か月間のメトホルミン投与でACF数は減少したが，血糖値，HbA1c，HOMA-IR，総コレステロール，中性脂肪は有意な変化は示さなかった(表4)．

4．メトホルミン投与による細胞増殖活性とアポトーシスの変化

メトホルミンによるACF抑制効果のメカニズムを解明するため直腸粘膜における細胞増殖活性を調べた．図10-A, Bのようにに PCNA labeling indexはメトホルミンの投与により有意に抑制されていた．一方，TUNEL法によるアポトーシスの変化は認めなかった(図10-C, D)．以上より，メトホルミンによるACF抑制は，細胞増殖の抑制効果による影響が示唆される．

メトホルミンを用いた癌の化学予防の展開

以上われわれの研究成果を紹介したが，実際メトホルミンで腸管で著明に糖の取り込みが亢進することから，メトホルミンを用いた化学予防は大腸癌で有効と思われる．われわれのfeasibility studyでは非糖尿病患者にわずか250mgのメトホルミンで有意な抑制効果を確認できた．この投与量では有害事象はまったく認めなかった．現在大腸腫瘍をエンドポイントとした試験を進行中である．

メトホルミンを用いた癌の化学予防は表5に示すように海外で多くの臨床試験が進行中であり，その結果が期待されている．

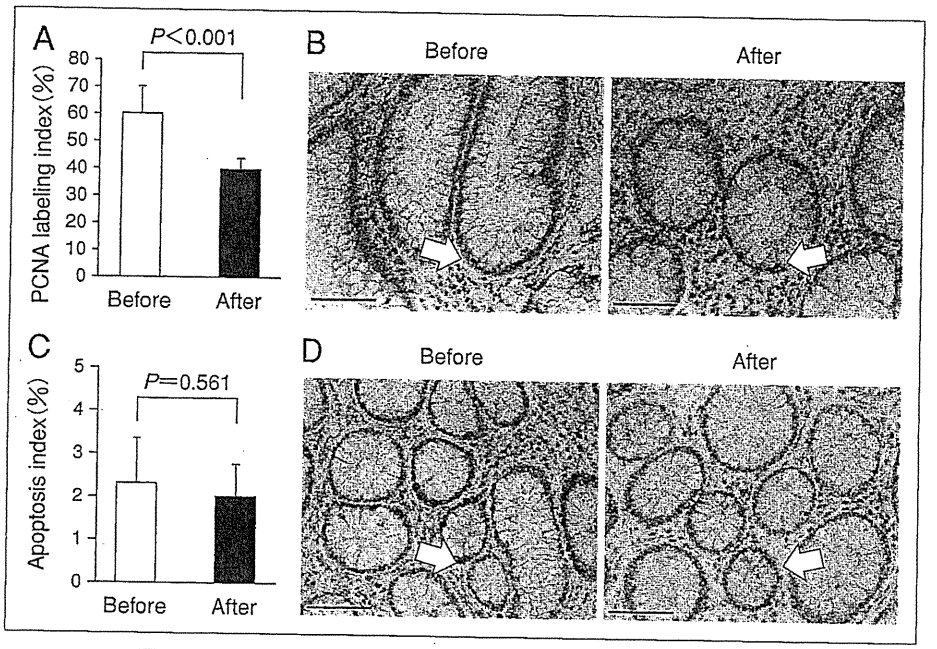

図10　メトホルミン群における細胞増殖活性とアポトーシスの評価
A：メトホルミン投与前後の平均PCNA labeling index．メトホルミンの投与で有意に抑制された．
B：PCNA免疫組織化学染色像．スケールバー：100μm．
C：メトホルミン投与前後の平均アポトーシスindex．2群間で有意差はなし．
D：TUNEL染色．矢印はTUNEL陽性シグナル．スケールバー：100μm．

表5　メトホルミンを用いたヒト癌を対象とした進行中の臨床試験

登録番号	タイトル	対象とする疾患
NCT00897884	Clinical and Biologic Effects of Metformin in Early Stage Breast Cancer	乳癌
NCT01087983	Lapatinib With Sirolimus or Metformin	さまざまな癌
NCT00984490	Metformin Hydrochloride in Treating Women With Stage I or Stage II Breast Cancer That Can Be Removed By Surgery	乳癌
NCT00881725	A Study of Pre-operative Metformin in Prostate Cancer (ANIMATE)	前立腺癌
NCT01101438	Metformin Hydrochloride in Treating Patients With Early-Stage Breast Cancer	乳癌
NCT00909506	Efficacy and Safety of Adjuvant Metformin for Operable Breast Cancer Patients	乳癌
NCT00930579	Metformin Pre-Surgical Pilot Study	乳癌

〔http://clinicaltrials.govより引用改変(2011年1月現在)〕

メトホルミン内服により癌の発生が明らかに低くなる疫学研究からメトホルミンで癌の化学予防が可能であると考えられる．しかしながら今後，投与量，どのような患者に投与するのか，投与期間，有害事象，投与時期，効果などまだまだ大腸癌一つをとっても検討すべきことが多々ある．メトホルミンによる大腸癌の化学予防はこれまでの医学の歴史が予防は治療に勝ることを考えると，非常に重要な課題であると考えられる．

文　献

1) Shaw RJ, Lamia KA, Vasquez D, et al. The kinase LKB1 mediates glucose homeostasis in liver and therapeutic effects of metformin. Science 2005 ; 310 : 1642.
2) Evans JM, Donnelly LA, Emslie-Smith AM, et al. Metformin and reduced risk of cancer in diabetic patients. BMJ 2005 ; 330 : 1304.
3) Bowker SL, Majumdar SR, Veugelers P, Johnson JA. Increased cancer-related mortality for patients

with type 2 diabetes who use sulfonylureas or insulin. Diabetes Care 2006 ; 29 : 254.
4) Hosono K, Endo H, Takahashi H, et al. Metformin suppresses azoxymethane-induced colorectal aberrant crypt foci by activating AMP-activated protein kinase. Mol Carcinog 2010 ; 49 : 662.
5) Zhou G, Myers R, Li Y, et al. Role of AMP-activated protein kinase in mechanism of metformin action. J Clin Invest 2001 ; 108 : 1167.
6) Martin DE, Hall MN. The expanding TOR signaling network. Curr Opin Cell Biol 2005 ; 17 : 158.
7) Gontier E, Fourme E, Wartski M, et al. High and typical ^{18}F-FDG bowel uptake in patients treated with metformin. Eur J Nucl Med Mol Imaging 2008 ; 35 : 95.
8) Hosono K, Endo H, Takahashi H, et al. Metformin suppresses colorectal aberrant crypt foci in a short-term clinical trial. Cancer Prev Res 2010 ; 3 : 1077.

* * *

大腸腺腫切除後の再発予測因子としてのaberrant crypt fociの検討

高橋　宏和，細野　邦広，中島　　淳

日本消化器がん検診学会雑誌
第49巻5号（210）2011　別冊

経 験

大腸腺腫切除後の再発予測因子としてのaberrant crypt fociの検討

高橋 宏和，細野 邦広，中島 淳
横浜市立大学附属病院 消化器内科

〔要 旨〕
大腸腺腫切除後の検査間隔や期間の指標に明らかなものは示されておらず，本研究では色素拡大内視鏡で観察し得る微小病変であるaberrant crypt foci（ACF）をサロゲートマーカーとし，大腸腺腫切除後の再発予測因子となりうるか検討した。当院において内視鏡的に切除可能であった大腸腺腫89例において下部直腸のACFを観察し，その数が0－3，4以上の2群に分類し，1年後大腸ポリープの発生の差を検討した。ACFの数は初回と比べ1年後に変化がなかった。1年後はACFの多い群において最大径が有意に大きかった。大腸腺腫切除後の再発予測においてACF数と腺腫の最大径が相関し，ACF数が腺腫再発の指標になることが示唆された。

キーワード aberrant crypt foci，大腸腺腫，サロゲートマーカー

はじめに

本邦において大腸がん罹患率は増加の一途をたどっており，今後がんの死因の第一位になると予想されている。大腸がんは早期に発見，治療すれば5年生存率が90％を超え根治が見込めるため，臨床の場において便潜血反応，注腸造影検査，大腸内視鏡検査などが積極的に行われている。大腸がんの早期診断として，大腸ポリープの既往，便潜血反応，家族歴などでハイリスクグループを絞り込み，これらに対し大腸内視鏡検査や注腸造影検査などが行われているが，多大な労力と医療費をかけるサーベイランスが大腸がんの罹患率や死亡率を減少させるか明確な答えは得られていない。本稿では色素拡大内視鏡で観察し得る微小病変であるaberrant crypt foci（ACF）をサロゲートマーカーとし大腸腺腫切除後の再発予測因子となりうるか検討した。

対象と方法

当院において内視鏡的に一括切除可能であった最大25㎜の大腸腺腫89例において下部直腸のACFを観察し（図1），その数が0－3，4以上の2群に分類し，1年後大腸ポリープの数および最大径を検討した。病理組織学的に大腸がんと診断された症例は除外した。ACFはメチレンブルーに濃染する通常より大きい腺窩で類円型，細隙型の形態をとる。次の病態は除外した。（大腸がんの既往歴，家族歴，炎症性腸疾患，放射性腸炎，NSAIDsもしくはアスピリン内服歴）

結果

ACFの多い群，少ない群の間に年齢，ウエスト周囲径，BMI，総コレステロール，中性脂肪，HbA1c，総脂肪面積，内臓脂肪面積，皮下脂肪面積の統計的有意差は認めなかった（表1）。ACFの数は初回と比べ1年後に変化がなかった。1年後はACFの多い群において最大径が有意に大きかった（表2）。

考案

ACFは1987年にBirdらによって化学発がんモデルマウスの大腸粘膜に見出された微小病変で，

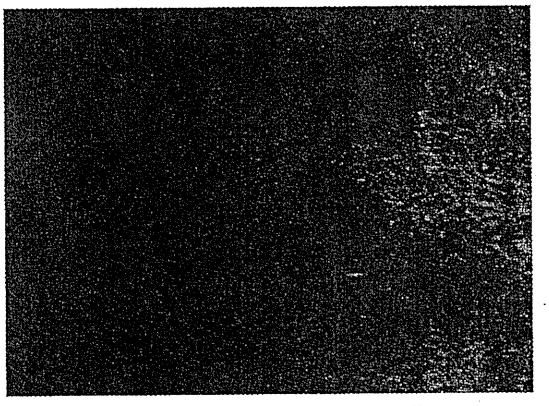

図1 ヒトACFの拡大内視鏡像
大腸がんのサロゲートマーカーとされるACFはメチレンブルーに濃染する微小病変で拡大内視鏡で観察される。

		ACF数		
	計	0-3	>3	*P*
症例数	89	41	48	
年齢(歳)	63.4 ± 11.1	62.6 ± 12.9	64.1 ± 9.5	0.52
性別(男:女)	61:28	28:14	33:15	
ウエスト周囲K(cm)	85.9 ± 11.5	84.7 ± 8.1	86.7 ± 13.6	0.57
BMI (kg/m^2)	23.2 ± 3.1	22.6 ± 2.3	23.8 ± 3.6	0.09
総コレステロール(mg/dl)	210.7 ± 34.9	208.7 ± 32.6	212.2 ± 36.9	0.69
中性脂肪(mg/dl)	146.2 ± 77.1	125.9 ± 64.1	161.5 ± 83.2	0.06
Hb A1c	5.9 ± 1.3	5.6 ± 1.2	6.2 ± 1.4	0.13
総脂肪面積(cm^2)	198.9 ± 95.2	177.0 ± 55.6	215.5 ± 115.2	0.19
内臓脂肪面積(cm^2)	90.4 ± 53.5	75.6 ± 41.1	101.6 ± 59.7	0.11
皮下脂肪面積(cm^2)	108.5 ± 58.1	101.4 ± 45.7	113.9 ± 66.4	0.49

表1 対象症例における生活習慣因子の比較

大腸腺腫やがんの前病変であることが確認されている[1),2)]。ヒトにおいても拡大内視鏡を用いることによりメチレンブルーに濃染するACFの観察が可能である[3)]。ヒトACFが大腸がんの前病変であるかは統一した見解はないが，モノクローナルな変化でありWntシグナル活性化やk-*ras*の変異が認められることから，近年の検討では代替指標(サロゲートマーカー)になるとされている[4)]。病変が微少であることが免疫組織学的解析を困難にする一因であるが，拡大内視鏡による存在診断は比較的容易である。これまでの検討では，ヒトACF数は内臓脂肪面積に相関しアディポネクチ

初回のACF数		0-3	>3	P
症例数		41	48	
初回	腺腫の数	1.4 ± 1.2	1.6 ± 1.8	0.71
	腺腫の最大径	6.0 ± 4.6	6.3 ± 7.2	0.81
1年後	腺腫の数	1.0 ± 1.0	1.5 ± 1.4	0.08
	腺腫の最大径	3.5 ± 3.5	5.5 ± 5.8	0.03*

表2 初回のACF数と1年後の腺腫発生

ンに逆相関した[5]，男性においてはIGF-1と相関した[6] 等の報告がされているが，本研究ではACF数の多い群と少ない群間に生活習慣因子の有意差は認められなかった。1年間の経過観察中にACF数の変化は認めなかったが，ACFの多い群においては最大径が大きくなることが示唆された。大腸腺腫切除後の経過観察期間についてガイドラインは示されておらず，ハイリスク群においては比較的短期間のうちに再検査を勧めることが多い。ACF数が大腸腫瘍発生の予測因子になりうるかさらなる検討が必要となる。

結語

大腸腺腫切除後の再発予測においてACF数と腺腫の最大径が相関し，ACF数が腺腫再発の指標になることが示唆された。今後増加が予想される大腸がんを減少させるためには，検診における精検受診率を上げることが重要である。リスクに合わせ，検査頻度や検査内容を選択できることが望ましくACFがその一助になることを期待する。

文　献

1) Bird RP: Observation and quantification of aberrant crypts in the murine colon treated with a colon carcinogen: preliminary findings. Cancer Lett 1987；37：147 - 151.

2) Pretlow TP, Barrow BJ, Ashton WS, et al：Aberrant crypts: putative preneoplastic foci in human colonic mucosa. Cancer Res 1991；5：1564 - 1567.

3) Takayama T, Katsuki S, Takahashi Y, et al：Aberrant crypt foci of the colon as precursors of adenoma and cancer. N Engl J Med 1998；339：1277 - 1284.

4) Stevens RG, Pretlow TP, Hurlstone DP, et al：Comment re："Sporadic aberrant crypt foci are not a surrogate endpoint for colorectal adenoma prevention" and "Aberrant crypt foci in the adenoma prevention with celecoxib trial". Cancer Prev Res 2008；1：215.

5) Takahashi H, Takayama T, Yoneda K, et al：Association of visceral fat accumulation and plasma adiponectin with rectal dysplastic aberrant crypt foci in a clinical population. Cancer Science 2009；100：29 - 32.

6) Takahashi H, Takayama T, Hosono K, et al：Correlation of the plasma level of insulin-like growth factor-1 with the number of aberrant crypt foci in male individuals. Mol Med Rep 2009；2：339 - 343.

論文受付　平成22年12月24日
同 受 理　平成23年4月27日

Relationship between human rectal aberrant crypt foci and the formation of colorectal polyps -One-year follow-up after polypectomy-

Hirokazu TAKAHASHI, Kunihiro HOSONO and Atsushi NAKAJIMA

Gastroenterology Division, Yokohama City University School of Medicine

Aberrant crypt foci (ACF) are the earliest detectable abnormality and precede adenomas. We wanted to determine the adenoma incidence over a 1-year period after polypectomy. Eighty-nine subjects were recruited from the population of Japanese individuals who underwent polypectomy at our institution. A total of 366 ACFs were identified in the 89 patients; all had baseline adenomas removed at the first colonoscopy examination and returned after 1 year. ACFs in the lower rectum were assessed at year 0, and the study group was divided into two groups depending on the number of ACFs: 0-3 ACFs in the first group and 4 or more ACFs in the second group. All participants were examined with regard to the number and maximum size of the adenomas. There was no statistical difference in the number and maximum size of the ACFs at year 0; however, the maximum size was larger in the 4-or-more group than in the 0-3 group at year 1. The meaning of the number of ACFs is not yet clear. However, the number of ACFs may be a predictive factor of the relatively large adenoma incidence in the pilot-phase study.

Keywords : aberrant crypt foci, colorectal adenoma, surrogate marker

OPEN ACCESS Freely available online

PLoS one

Onset of Quiescence Following p53 Mediated Down-Regulation of H2AX in Normal Cells

Yuko Atsumi[1☯], Hiroaki Fujimori[1,3☯], Hirokazu Fukuda[2☯], Aki Inase[2], Keitaro Shinohe[3], Yoshiko Yoshioka[3], Mima Shikanai[3], Yosuke Ichijima[3], Junya Unno[4], Shuki Mizutani[4], Naoto Tsuchiya[2], Yoshitaka Hippo[2], Hitoshi Nakagama[2], Mitsuko Masutani[1], Hirobumi Teraoka[3], Ken-ichi Yoshioka[1,3]*

1 Division of Genome Stability Research, National Cancer Center Research Institute, Tokyo, Japan, **2** Division of Cancer Development System, National Cancer Center Research Institute, Tokyo, Japan, **3** Department of Pathological Biochemistry, Medical Research Institute, Tokyo Medical and Dental University, Tokyo, Japan, **4** Department of Pediatrics and Developmental Biology, Graduate School of Medical and Dental Sciences, Tokyo Medical and Dental University, Tokyo, Japan

Abstract

Normal cells, both *in vivo* and *in vitro*, become quiescent after serial cell proliferation. During this process, cells can develop immortality with genomic instability, although the mechanisms by which this is regulated are unclear. Here, we show that a growth-arrested cellular status is produced by the down-regulation of histone H2AX in normal cells. Normal mouse embryonic fibroblast cells preserve an H2AX diminished quiescent status through p53 regulation and stable-diploidy maintenance. However, such quiescence is abrogated under continuous growth stimulation, inducing DNA replication stress. Because DNA replication stress-associated lesions are cryptogenic and capable of mediating chromosome-bridge formation and cytokinesis failure, this results in tetraploidization. Arf/p53 module-mutation is induced during tetraploidization with the resulting H2AX recovery and immortality acquisition. Thus, although cellular homeostasis is preserved under quiescence with stable diploidy, tetraploidization induced under growth stimulation disrupts the homeostasis and triggers immortality acquisition.

Citation: Atsumi Y, Fujimori H, Fukuda H, Inase A, Shinohe K, et al. (2011) Onset of Quiescence Following p53 Mediated Down-Regulation of H2AX in Normal Cells. PLoS ONE 6(8): e23432. doi:10.1371/journal.pone.0023432

Editor: Michael Polymenis, Texas A&M University, United States of America

Received April 11, 2011; **Accepted** July 17, 2011; **Published** August 12, 2011

Funding: This study was supported by MEXT KAKENHI (20770136 and 20659047). The funders had no role in study design, data collection and analysis, decision to publish, or preparation of the manuscript.

Competing Interests: The authors have declared that no competing interests exist.

* E-mail: kyoshiok@ncc.go.jp

☯ These authors contributed equally to this work.

Introduction

Cancer is a disease associated with genomic instability and the accumulation of mutations [1]. Unlike specific chromosomal translocation-associated tumors, most cancers associated with aging develop either chromosomal instability (CIN) or microsatellite instability (MIN) [2]. While MIN is associated with mismatch repair deficiency, CIN develops even in a normal background [3]. However, the mechanisms by which CIN and MIN develop remain elusive.

A recent genomic analysis of various cancers revealed that massive genomic rearrangements, including loss of heterozygosity (LOH) and chromosomal translocation, amplification and deletion, do not gradually accumulate over time, as conventionally thought, but appear to be acquired in a single catastrophic event [4]. One of such events could be associated with tetraploidization because tetraploidy is a common early event in cancer cells with CIN [5]. Tetraploidy is observed in cells during the initial stages of cancer [6,7] as well as in precancerous stages such as dysplasia [8,9], but not in malignant cancer cells, which usually exhibit aneuploidy in association with deploidization [5]. Furthermore, analogous to changes observed in cancer genomes, the immortalization of mouse embryonic fibroblasts (MEFs) occurs with tetraploidy and mutation of the Arf/p53 module, which eventually evolves into aneuploidy during serial cultivation [10].

In the initial stages of carcinogenesis, cells are subjected to oncogenic stress, resulting in the accumulation of DNA replication stress-associated lesions and the onset of barrier responses such as senescence and apoptosis [11,12]. This effect can be reproduced *in vitro* by the activation of oncogenes [11] and accelerated growth stimulation [12] due to the induction of accelerated S-phase entry and the resulting DNA replication stress. Importantly, genomic instability is generated under these conditions [11,12] because DNA replication stress-associated lesions persist into M phase and mediate chromosomal bridge formation and cytokinesis failure, resulting in tetraploidization [10]. In fact, tetraploidization of MEFs is induced via chromosomal bridge formation prior to the onset of immortality with mutation of Arf/p53 [10], although it is still unclear how tetraploidization induces immortality. Since such tetraploidization is specifically observed during senescence, tetraploidization might be a defect that occurs during cell proliferation or growth arrest. In fact, similar to cells in the initial stages of carcinogenesis, senescent cells often accumulate irreparable DNA lesions [13,14] and frequently exhibit genomic instability [15].

The development of cancer, as well as the onset of immortality in cells *in vitro*, is tightly associated with mutations in the Arf/p53 module [16–18]. Although this is ascribed to the role of p53 in

cancer prevention, the regulation and roles of p53 are complex [18]. While constitutively active p53 mediates premature aging in mice [19–21], additional single gene copies of *Arf* and *p53* under functional regulation mediate longevity and cancer prevention [22]. Similarly, while the accumulation of p53 induces cellular senescence and apoptosis [16,17], additional single gene copies of *Arf* and *p53* in MEFs has a protective effect from immortalization [22], suggesting that they help to maintain homeostasis under undamaged conditions. This raises the questions of the identity of the regulatory target of p53 in preserving cellular homeostasis under normal conditions and how cellular homeostasis preservation and abrogation are associated with genomic status and p53 regulation.

This study focused on the mechanism by which normal cells under serial proliferation regulate homeostasis preservation and abrogation and sought to identify the regulatory target of p53. Our results illustrated two distinct conditions that could result in growth-arrested cells: (i) cells that maintain continuous quiescence by down-regulating H2AX (a variant of core histone H2A) under p53 regulation and stable-diploidy maintenance; and (ii) cells that develop tetraploidy and immortality under continuous growth stimulation, characterized by the accumulation of γH2AX foci. Thus, oncogenic stress under growth stimulation triggers catastrophic tetraploidization that leads to immortalization in association with the accompanying mutation of the Arf/p53 module and recovery of H2AX expression and growth activity.

Results

Immortality is prevented in quiescent cells that maintain genomic stability

MEFs cultured under the standard 3T3 protocol (Std-3T3) senesce in association with oxygen sensitivity [23], which is followed by the development of immortality with tetraploidy [10] and mutation of the Arf/p53 module [22], similar to the process of carcinogenesis. In addition, similar to cells in the initial stages of carcinogenesis, spontaneous DNA lesions accumulate in senescent MEFs under Std-3T3 conditions prior to the development of immortality [10], which suggests that growth stimulation induced under Std-3T3 conditions might overwhelm senescent MEFs. Therefore, MEFs under Std-3T3 conditions were compared with MEFs exposed to temporary serum deprivation (tSD-3T3), which induces occasional growth arrest (Fig. 1A). Under Std-3T3 conditions, MEFs were immortalized with tetraploidy that progresses to aneuploidy (Fig. 1A–C). On the other hand, MEFs cultured under tSD-3T3 conditions never developed immortality and preserved quiescence with stable diploidy (Fig. 1A, C). This indicates that temporal growth arrest prevents immortalization and supports genomic stability. Conversely, continuous culture with 10% FBS produces oncogenic stress in senescent MEFs, triggering tetraploidization. Thus, even though both are growth arrested (at least in total cell numbers) with senescent morphology at the same culture passage (P9) (Fig. S1), MEFs under tSD-3T3 conditions are continuously quiescent with genomic stability, while MEFs under Std-3T3 conditions develop tetraploidy (Fig. 1A, C), posing a question in DNA lesion status that induces chromosomal bridge formation and tetraploidization [10].

γH2AX foci accumulate in cells developing genomic instability but not in cells preserving diploidy

To determine the DNA lesion status induced by accelerated growth stimulation, γH2AX foci were compared in growth-arrested MEFs (P9) under both conditions (Fig. 1D). As expected, MEFs that developed tetraploidy under Std-3T3 conditions accumulated γH2AX foci, with some carrying over into the G2/M phases (Fig. 1E). This resulted in chromosome bridge formation (Fig. 1F) with the resulting tetraploidization that is initially observed with binucleated tetraploidy (Fig. 1F). On the other hand, quiescent MEFs that preserved genomic stability under tSD-3T3 conditions did not develop γH2AX foci (Fig. 1D), indicating that genomic stability is preserved under no γH2AX signal. However, it was still unclear why quiescent MEFs under tSD-3T3 conditions do not accumulate γH2AX foci because senescent cells are known to generally accumulate irreparable DNA lesions [13,14].

To address why γH2AX foci do not form under tSD-3T3 conditions, the expression level of H2AX at P9 was determined. As shown in Figure 1G, a remarkable reduction in H2AX expression was observed in quiescent MEFs at P9 while MEFs that developed tetraploidy under Std-3T3 conditions showed significantly higher H2AX expression than quiescent MEFs. This illustrates an association between H2AX levels and the cellular and genomic status, in that cells with largely diminished H2AX expression preserve stable diploidy and a quiescent status, while cells with residual H2AX expression and with γH2AX foci develop genomic instability and immortality (Fig. 1H). Importantly, H2AX-KO cells exhibited impaired DNA repair, growth retardation, and elevated genomic instability [24–28], phenotypes reminiscent of senescent cells. Therefore, it will be critical to determine how H2AX-status is regulated to produce quiescence and induce genomic instability.

H2AX is generally diminished in quiescent cells

To address whether H2AX diminution is a general occurrence, H2AX expression was compared in normal human fibroblasts (NHFs) and MEFs. Decreased H2AX was observed in both cell types at growth-arrested stage after serial proliferation (Fig. 2A, B), suggesting that this process is conserved between humans and mice. In addition, H2AX diminution was also observed in many organs of adult mice, including the liver, spleen, and pancreas (Fig. 2C, D; Fig. S2). Thus, H2AX is generally reduced in quiescent cell chromosomes both *in vitro* and *in vivo*.

H2AX is also diminished during premature senescence induced by DNA damage. Using early passage MEFs (P2), H2AX diminution was observed when senescence was induced by treatment with hydroxyurea (HU) to induce DNA replication stress (Fig. 2E) and with the radiomimetic DNA-damaging agent, neocarzinostatin (Fig. S3). This most likely occurs because DNA repair is coupled with H2AX release and chromatin remodeling [29–31]. Together with results showing a decrease in H2AX transcript levels in senescent MEFs (Fig. S4), these results indicate that decreased amounts of H2AX protein in senescing cells is ascribed to a decrease in H2AX transcript levels and DNA damage.

To directly address the impact of H2AX reduction, H2AX was knocked down in early passage NHFs, which induced cellular quiescence with senescent cell characteristics; cells adopted a flattened and enlarged morphology and showed an increase in senescence-associated β-galactosidase activity (Fig. 2F). Since the knockdown of H2AX in 293T cells induced growth arrest without inducing a senescent morphology (data not shown), it is likely that the effect of H2AX diminution is primarily due to quiescence induction and potentially a normal consequence of senescence in normal cells.

Immortalized cells develop following tetraploidization when H2AX status and growth activity are restored

The above results illustrate that cellular quiescence is produced when cells maintain stable diploidy and diminished H2AX

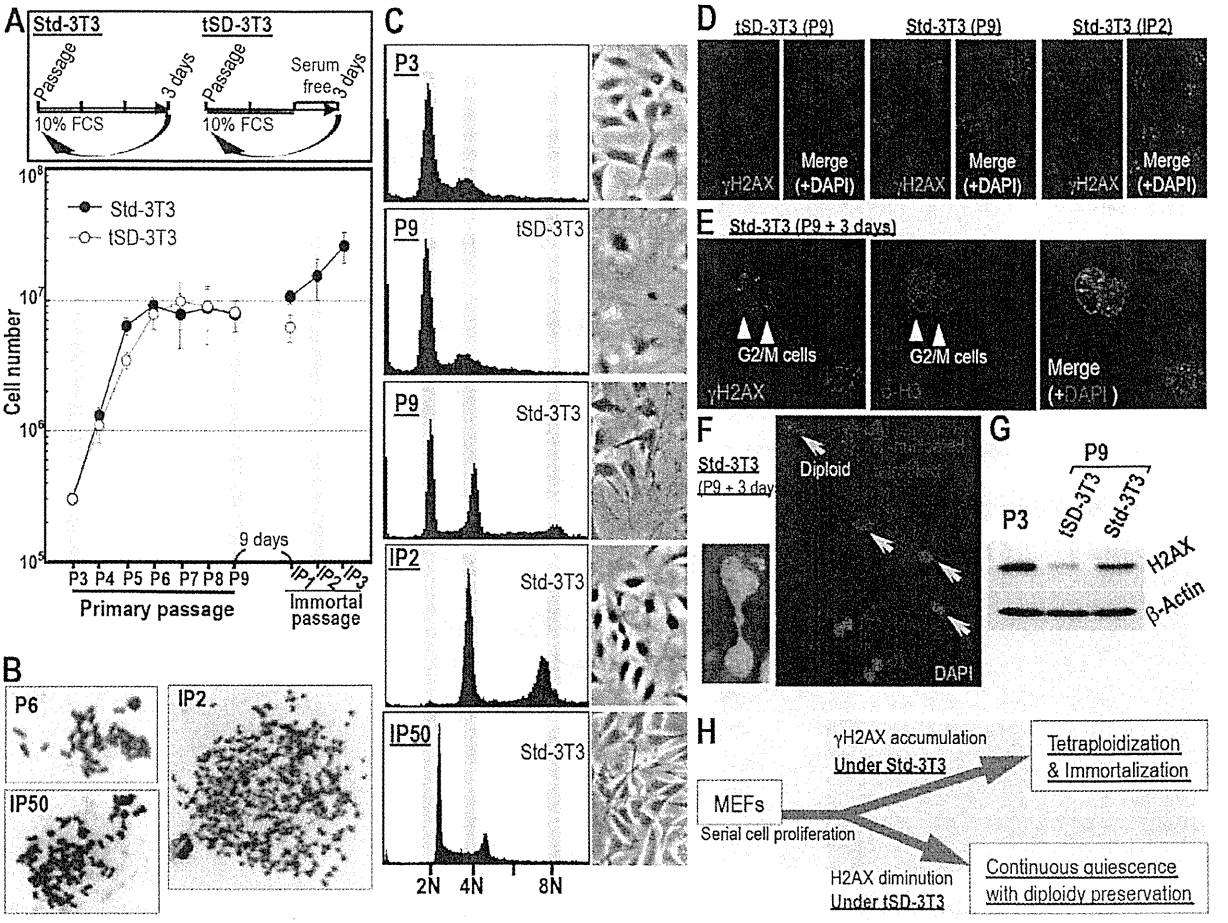

Figure 1. Immortality with tetraploidy is blocked in quiescent cells with diploidy, diminished H2AX, and no γH2AX foci. A. Growth curves of MEFs cultured under the standard 3T3 protocol (Std-3T3) or the T3 protocol with temporary serum deprivation (tSD-3T3) as schematically shown. MEFs under Std-3T3 conditions were immortalized, whereas MEFs cultured under tSD-3T3 conditions were not. **B** Genomic instability developed in immortalized MEFs (IP2) under Std-3T3 conditions. **C.** Genomic status was determined by flow-cytometry at the indicated conditions and passages. Representative images are shown. Tetraploidy development was blocked under tSD-3T3 conditions, while tetraploidy had already developed in growth-arrested MEFs at P9 under Std-3T3 conditions (see increasing 4N and 8N peaks). **D.** DNA lesions identified by γH2AX foci spontaneously accumulated in MEFs developing tetraploidy and immortality (P9) under Std-3T3 conditions as well as in immortal cells (IP2), while MEFs that maintained quiescent status with genomic stability under tSD-3T3 conditions contained no foci. **E.** DNA lesion-carryover into the G2-M phases was determined for lesions that spontaneously accumulated in senescent MEFs under Std-3T3 conditions. DNA lesions in senescing MEFs are also observed in the G2-M phases determined by phosphorylated H3. **F.** Chromosome bridge formation (Left panel) is observed in association with DNA lesion-carryover into the G2-M phases under Std-3T3 conditions with the resulting accumulation of bi-nucleated tetraploidy (Right panel: red arrow heads). Representative images are shown. **G.** The total H2AX level at P9 under each condition was determined. Whereas a significant reduction in H2AX expression was observed in MEFs with genomic stability under tSD-3T3 conditions, MEFs that developed immortality and genomic instability under Std-3T3 conditions did not show a significant decrease in H2AX expression. **H.** A model of the life-cycle of MEFs undergoing quiescence or developing immortality. While quiescent MEFs preserve diploidy and show diminished H2AX levels, MEFs developing immortality exhibited γH2AX foci accumulation.

doi:10.1371/journal.pone.0023432.g001

expression. In these cells, the H2AX level is less than 100-fold compared to that in actively growing cells. To study the effect of growth stimulation in cells with an H2AX-diminished quiescent status, complete medium (DMEM with 10% FBS) was added to quiescent MEFs prepared under tSD-3T3 conditions (Fig. 3A–C). In these cells, cell-cycle progression was initiated with the expression of PCNA and histones H3 and H2AX, which led to γH2AX foci formation (Fig. 3D, E). Abrogating quiescent status with complete medium resulted in the establishment of immortalized MEFs with tetraploidy (Fig. 3A–C). However, it took 30 days to initiate immortal passage in H2AX-diminished quiescent MEFs, while immortality was acquired in only 9 days for P9 MEFs under Std-3T3 conditions, suggesting that the H2AX-diminished quiescent status protected cells from immortalization. Supporting this argument, primary MEFs transfected with an H2AX expression vector also acquired immortality at an accelerated rate (Fig. S5A–C). Such H2AX-overexpression may induce the effect of DNA replication stress because immortality in H2AX-overexpressing MEFs were again developed with tetraploidy (Fig. S5D,E). Unexpectedly, H2AX status was totally recovered in actively growing, immortalized MEFs (Fig. 3F, G), which illustrates the association of H2AX status with growth activity.

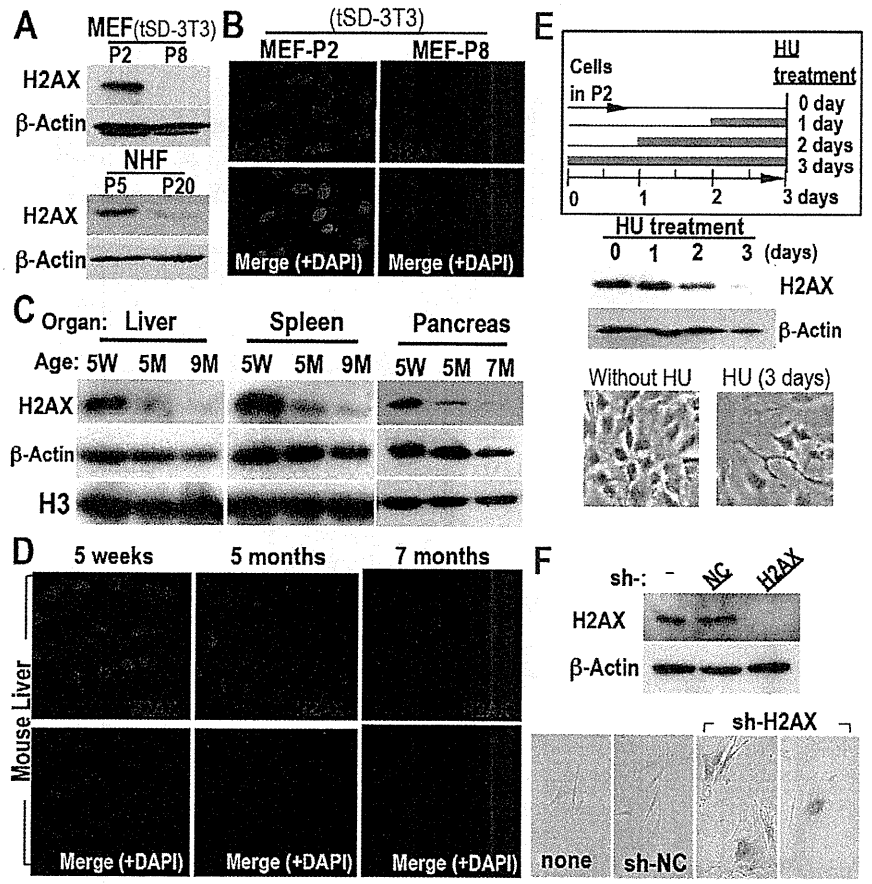

Figure 2. Quiescent cell-status is induced with H2AX diminution both *in vitro* and *in vivo*. A,B H2AX expression in growth-arrested cells (P8 for MEFs under tSD-3T3 conditions, P20 for NHFs) was determined by Western blotting (**A**) and immunofluorescent staining (**B**), revealing H2AX diminution in both types of growth-arrested cells. **C,D** H2AX diminution was also measured in adult mice organs by Western blotting (**C**) and in liver sections by immunofluorescent staining (**D**). Samples were prepared from five week (5W), five month (5M) and seven- or nine-month-old mice (7M or 9M). **E.** The involvement of H2AX diminution in DNA damage-induced premature senescence was determined after 0.2 mM HU treatment. Orange bars indicate the periods of HU treatment. Premature damage-induced senescence was observed with H2AX diminution, in which cells were flattened and enlarged, morphology typical of senescent cells. **F.** The effect of H2AX knockdown on senescence was determined in NHFs. Senescence was directly induced by H2AX knockdown in NHFs. H2AX status and senescence was determined by Western blotting (top) and SA-β-gal activation, and cells exhibited a flattened and enlarged morphology (bottoms), respectively.
doi:10.1371/journal.pone.0023432.g002

However, this also poses the question of how the down-regulation of H2AX expression in quiescent MEFs is reversed after immortalization.

Immortalized cells no longer achieve H2AX diminution-associated quiescent status

To explore the effects of the change in H2AX status, the response of H2AX to DNA replication stress was compared between primary and immortalized MEFs. While H2AX in primary MEFs was down-regulated after HU treatment, this did not occur in immortalized MEFs (Fig. 3H), which indicates that H2AX diminution-associated quiescent cell status is not inducible after immortalization. Thus, quiescent status is preserved in cells with diminished H2AX expression and stable diploidy but is abrogated under continuous growth stimulation, inducing cell cycle progression and γH2AX foci formation, and eventually leading to immortality with tetraploidy and H2AX recovery. Since the Arf/p53 module is specifically mutated during MEF immortalization [22], p53 might be involved in H2AX down-regulation. In fact, unlike senescent normal cells, H2AX expression is relatively high (2–20% of total H2A) in cancer cells as well as in growing NHFs (10%) [28].

H2AX diminution-associated quiescent status is produced by p53 and prohibits the development of immortality

To determine the involvement of p53 in H2AX down-regulation, *p53* knockout (KO) MEFs were cultured. Unlike normal primary MEFs, but similar to immortalized MEFs (Fig. 3H), H2AX expression in primary *p53*-KO-MEFs was not decreased by HU treatment (Fig. 4A). Furthermore, *p53*-KO-MEFs continuously grew, without change in H2AX status even under tSD-3T3 conditions (Fig. 4B, C). This indicates that H2AX in wild-type (WT)-MEFs is down-regulated by p53 to

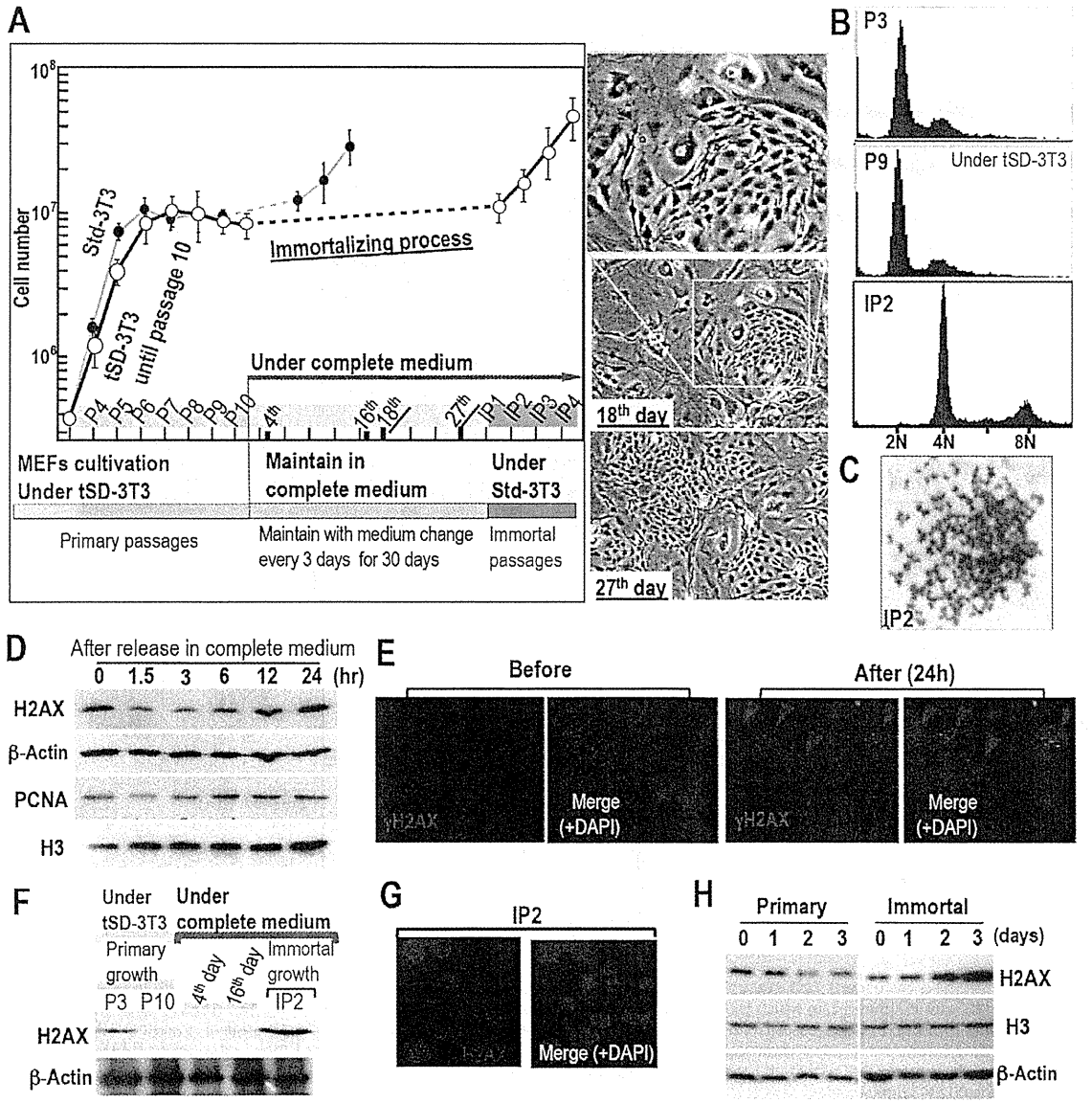

Figure 3. H2AX-diminished quiescent cell-status is abolished by continuous growth stimulation with accompanying H2AX recovery. A. Quiescent MEFs with diminished H2AX expression were cultured under tSD-3T3 conditions until P10. They were then exposed to complete medium, which was changed every three days for 30 days. Immortal passages were started under Std-3T3 conditions (red circles). MEFs cultured under the Std-3T3 conditions (black circles) as in Figure 1a were superimposed for comparison of the time needed to acquire immortality. Representative images of MEFs during the process of acquiring immortality are also shown. **B,C.** Tetraploidy development in immortalized MEFs (IP2) was observed by flow-cytometry (**B**) and Giemsa staining (**C**). **D.** Growth acceleration-associated cell cycle progression and H2AX induction. To determine the effect of serum induction on H2AX expression and cell cycle progression, senescent MEFs at P8 were incubated in serum-free medium for 24 h and harvested after exposure to complete medium for various times. H2AX expression increased with increasing PCNA and histone H3, which suggests that the expression of these chromatin factors was associated with S phase entry. To detect H2AX levels in these MEFs at P8, the H2AX signal was visualized by longer exposure. **E.** DNA lesions characterized by γH2AX foci were induced in MEFs (red arrowheads) after exposure to complete medium as in **D. F,G.** H2AX status in immortalized MEFs was determined by Western blotting (**F**) and immunofluorescence (**G**), revealing H2AX recovery. **H.** DNA replication stress-associated H2AX diminution was compared between normal and immortalized MEFs as in Figure 2E, in which H2AX was not down-regulated after immortalization.
doi:10.1371/journal.pone.0023432.g003

induce cellular quiescence and is recovered in immortalized MEFs in association with tetraploidization and mutation of the Arf/p53 module. Although *p53*-KO-MEFs did not undergo H2AX diminution-mediated growth arrest, these MEFs still exhibited a senescent morphology (Fig. 4D, see P8) and subsequently achieved an immortalized morphology (P14), which suggests the immortalization of *p53*-KO-MEFs via the senescent stage without growth arrest. This also indicates that a quiescent cell status is induced by p53 to protect cells from immortality.

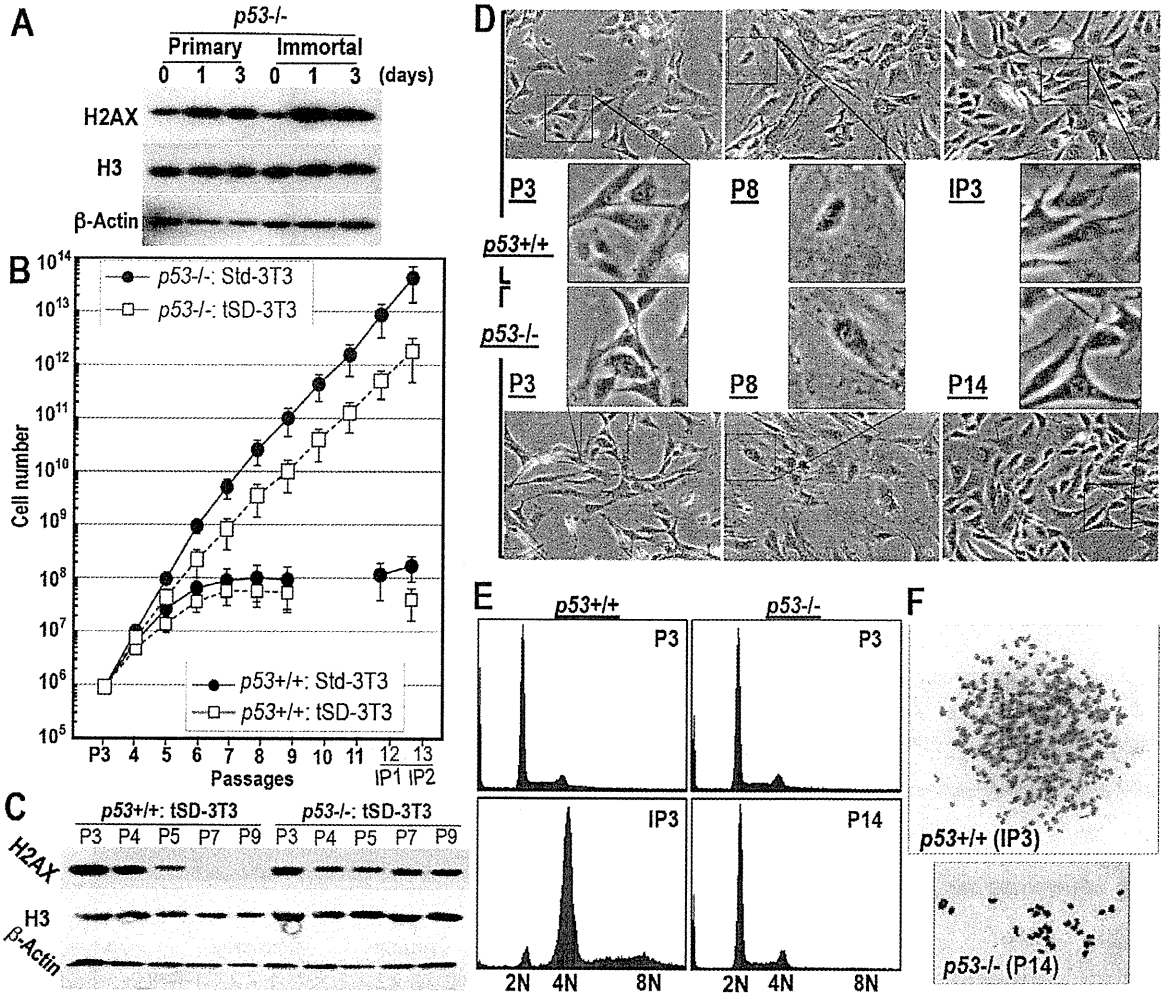

Figure 4. H2AX-diminished quiescent cell status is regulated by p53. A. DNA replication stress-associated H2AX diminution status was determined in *p53*-KO MEFs as in Figure 2E, in which H2AX was not down-regulated, even in primary MEFs. **B–F.** Primary *p53*-KO MEFs were cultured during the senescing and immortalizing processes (**B**). H2AX status was determined by Western blotting (**C**), morphological assessment (**D**), genomic status determined by flow-cytometry (**E**), and chromosome spread (**F**). Although *p53*-KO MEFs never showed major changes in H2AX expression, tetraploidization or growth arrest, *p53*-KO MEFs still exhibited a senescent morphology (P8) before achieving an immortalized morphology (P14).
doi:10.1371/journal.pone.0023432.g004

Mutation of the Arf/p53 module is induced with tetraploidization, triggered by DNA replication stress under moderately decreased H2AX levels in normal cells

Whereas *p53*-KO-MEFs are immortalized with diploidy (Fig. 4E, F), WT-MEFs are never immortalized only after tetraploidization [10] (Fig. 1B, C; Fig. 3B, C; Fig. 4E, F) and loss of Arf/p53 [22]. This suggests that the mutation of the Arf/p53 module in WT-MEFs is induced during tetraploidization. Supporting this argument, p53-dependent quiescence produced by diminished H2AX is maintained under diploidy preservation but abrogated after tetraploidization with mutation in the Arf/p53 module and the resulting H2AX recovery (Fig. 3). Therefore, normal WT-MEFs are protected from immortalization by a quiescent cell status, as long as the genome is preserved in diploidy. However, under continuous growth stimulation, tetraploidization also spontaneously arises in WT-MEFs but, unexpectedly, not in *p53*-KO-MEFs.

As tetraploidization was observed at the senescent stage under conditions of continuous growth stimulation that induce DNA replication stress (Fig. 3), the underlying reason for tetraploidization in WT-MEFs but not in *p53*-KO-MEFs might be associated with the repair deficiency that also occurs in an H2AX-diminished background. To examine the tetraploidization risk under an H2AX-diminished background, MEFs of each type were treated with HU for 36 hours and the incidence of bi-nucleated tetraploidy formation was compared (Fig. 5A). As expected, HU treatment-associated H2AX diminution (Fig. 2E) resulted in tetraploidization in primary WT-MEFs but not in immortalized WT-MEFs or p53-KO-MEFs (Fig. 5A). Thus, although normal cells become quiescent with largely diminished H2AX under diploidy, senescing cells with residual H2AX under growth stimulating conditions are potentially at risk of developing tetraploidy in response to DNA replication stress.

Finally, to address changes in DNA replication stress-sensitivity during serial proliferation of normal MEFs, the repair efficiencies

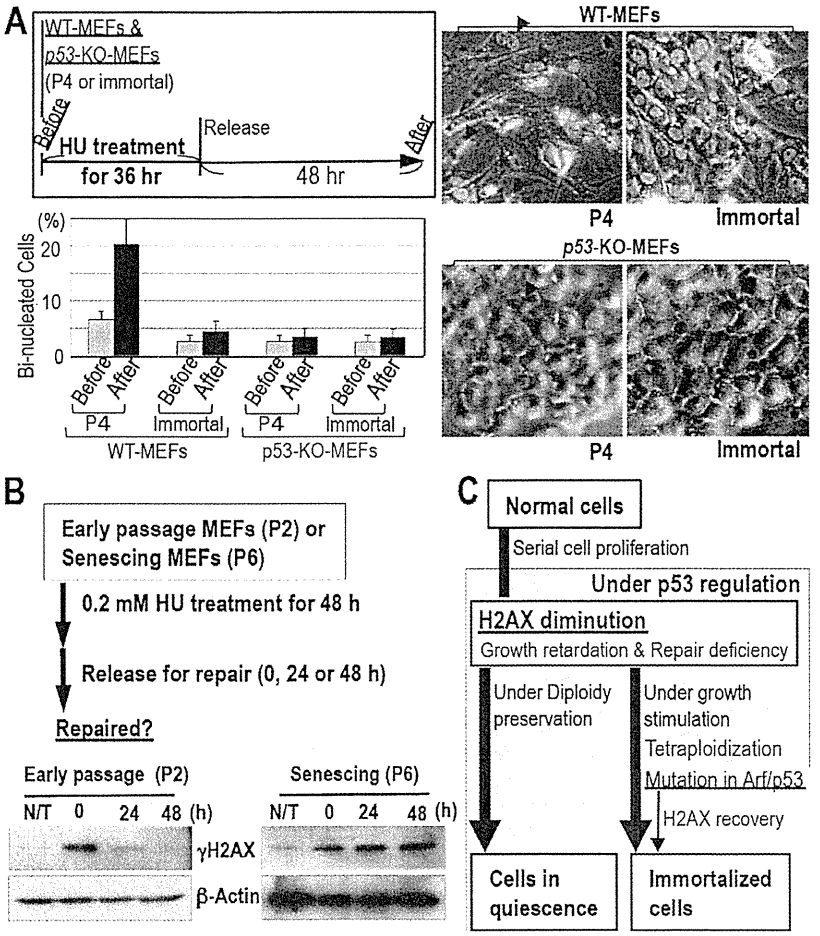

Figure 5. Increased risk of tetraploidization in normal MEFs. A. DNA replication stress-associated tetraploidization was determined in MEFs (P4) with the formation of bi-nucleated tetraploidy (red arrowhead) after 0.2 mM HU treatment as illustrated (top-left panel). Tetraploidization was efficiently induced during primary growth but not in immortalized MEFs or *p53*-KO-MEFs. **B.** Repair efficiencies of DNA replication stress-associated lesions were compared between early passage (P2) and senescing MEFs (P6) after 48 h hydroxyurea (HU) treatment. γH2AX signal was used as a marker of DNA lesions, in which γH2AX signal and β-Actin signals in senescing MEFs (P6) were detected only with over-exposure compared to early passage MEFs (P2), due to decreased H2AX levels during senescence. The reduction in γH2AX signal after release was only evident in early passage MEFs, which suggests that senescing cells are defective in resolving DNA replication stress. **C.** A model of MEFs under serial cell proliferation either undergoing quiescence or developing immortality. While MEFs that maintain quiescence and diploidy show diminished H2AX levels, MEFs developing immortality accumulate γH2AX foci.
doi:10.1371/journal.pone.0023432.g005

of DNA replication stress-associated lesions were compared between early passage and senescent MEFs with the decay of the γH2AX signal after release from HU treatment (Fig. 5B). Unlike early passage MEFs (P2), senescing MEFs (P6) were deficient in repairing HU-associated DNA lesions (Fig. 5B), in which MEFs show slow cell-cycle progression and residual H2AX expression. This is in contrast to quiescent MEFs with largely diminished H2AX level that show neither detectable cell cycle progression nor DNA replication stress. Thus, normal cells under serial proliferation decrease H2AX expression; thereby, cells slow growth activity and become defective in DNA repair. In such cells, cellular homeostasis is preserved by quiescence under largely diminished H2AX level regulated by p53 as long as diploidy is preserved. However, these cells are simultaneously at increased risk of tetraploidization with p53 dysfunction under continuous growth acceleration, resulting in the development of immortality and recovery of H2AX activity and cell growth (Fig. 5C).

Discussion

The results of this study revealed the following novel concepts: (i) normal cells generally achieve quiescent status with diminished H2AX level both *in vitro* and *in vivo*, and this is regulated by p53; (ii) growth arrested normal cells with senescent morphology can be defined as either (a) those in a continuous quiescent status with largely diminished H2AX level or (b) those in a transient status with inducing genomic instability and the resulting onset of immortality, under which cells accumulate γH2AX foci; (iii) to protect cells from immortality, one of the critical roles of p53 is the induction of growth-arrest via the down-regulation of H2AX with cellular quiescence. Cells in H2AX diminution-associated quiescence are shown in the cause of mature and premature senescence, during which cells show senescent morphology (Fig. S1), probably because these cells are repair defective (Fig. 5B). However such repair deficiency is also associated with genomic instability

development under accelerated growth stimulation, resulting in immortality acquisition with Arf/p53 module mutation and H2AX recovery.

Since growth-arrested cellular status with senescent morphology is directly induced by H2AX-knockdown (Fig. 2F), H2AX down-regulation is involved in a cause of quiescent cellular status. On the other hand, residual H2AX-expression in senescent cells is an associated effect for tetraploidization and immortalization: residual H2AX in senescent cells are only observed under accelerated growth stimulation (Figs. 1 and 3), under which cells are subjected to DNA replication stress and exhibit γH2AX, resulting in tetraploidization. Thus, even though cells are morphologically senescent with no growth in total cell number, cellular statuses could be either cells developing genomic instability under continuous growth acceleration (Std-3T3) or continuously quiescent cells under occasional arrest (tSD-3T3).

Unlike highly accumulated p53 that induces apoptosis, the Arf/p53 module under normal conditions functions for longevity by suppressing tumors in mice and giving protection from immortalization in MEFs [22]. Here, our results illustrated that such cellular status is produced with H2AX diminution-associated quiescence by protecting from immortalization under normal p53 regulation but is abrogated by Arf/p53 module mutation that is induced with tetraploidization under continuous growth stimulation, resulting in recovery of H2AX and growth activity. Unlike cells undergoing apoptosis, cells preserving quiescence under normal conditions do not accumulate p53 protein [10], which is probably associated with p53 function expression for quiescent status preservation but not for apoptosis induction. Intriguingly, such p53-dependent H2AX diminution was only observed after cells reach growth arrest both *in vivo* and *in vitro* but not growing cells in early passages and in organs from young mice (Fig. 2). In accordance with this, the expression of p53 targets Sidt2 and Phlda3, which are likely associated with tumor suppression [32], were elevated after cells become H2AX diminution-associated quiescent (P7) compared to cells in early passage (P3) (Fig. S6). However, similar to p53 protein, the increase in p53 transcript is also limited (Fig. S6). Thus, p53 function is expressed for apoptosis with accumulated p53, otherwise for H2AX-diminution associated quiescent status preservation under normal regulation without accumulating p53.

Except for tumors associated with specific chromosomal translocation, development of most cancers as well as *in vitro* cellular transformation is associated with genomic instability of either CIN or MIN [2,3]. Importantly, tetraploidization, a major initial form of CIN under a mismatch repair proficient background is induced with oncogenic stress by accelerated S-phase entry [10], leading to immortality acquisition in MEFs with mutation in the Arf/p53 module. Here, our results showed that quiescence could be preserved with largely diminished H2AX and diploidy preservation under the regulation of p53. Although H2AX down-regulation is only observed under functional p53 regulation, it is still unclear how p53 down-regulates H2AX. Our results showed the reduction of total H2AX transcript during the senescing process (Fig. S4) and a damage-induced decrease of H2AX protein under functional p53 regulation (Fig. 2E; Fig. 4A, B). Although p53 role for H2AX down-regulation is unclear, the regulation might be indirect because (1) there is no p53-binding site on the *H2AX* promoter, (2) there is no signal of the *H2AX* gene with ChIP-on-CHIP analyses against p53 [33], (3) H2AX expression does not associate with the activation level of p53 as we observed no association between H2AX expression and p53 activation (Fig. S7).

Together, our results provide a rationale for the regulation of cellular homeostasis preservation. By prohibiting immortality development and preserving quiescent cell status, p53 induces an H2AX diminution-mediated quiescent status. However, this status is abrogated by continuous growth stimulation, which results in the induction of genomic instability with mutation of the Arf/p53 module, which leads into H2AX recovery, the restoration of growth activity, and immortality acquisition (Fig. 5C).

Methods

Ethics Statement

Mice were treated in accordance with the Japanese Laws and the Guidelines for Animal Experimentation of National Cancer Center. All experiments were approved by The Committee for Ethics in Animal Experimentation of National Cancer Center (approval ID numbers: A59-09 and T07-038).

Cell culture and tissue samples

Cells were cultured as described previously [34]. Both wild-type and *p53*-KO MEFs were prepared from day 13.5 embryos of wild type and $p53^{(+/-)}$ mice [35] as previously described [34] and cultured under the standard 3T3 (Std-3T3) passage protocol [36] or with the following modifications: tSD-3T3. Senescing MEFs (P6 or P8) were maintained under tSD-3T3 conditions for the experiments shown in Figures 2, 3, 4, 5. NHFs (normal human umbilical cord fibroblasts; HUC-F2, RIKEN BRL Cell Bank) were cultured under Std-3T3 conditions. Resveratrol treatment of NHFs was performed as for MEFs. For the H2AX shRNA study, the reported sequence oligonucleotide [37,38] was inserted into the pSuper.retro.puro vector (Oligoengine) and the shRNA virus was then prepared using 293T cells. The virus was infected into NHF cells and selected with puromycin. Mouse tissue samples were prepared from mice at the ages indicated (Sankyo Labo Service).

DNA damage and induction of replication stress

DSB damage was induced by neocarzinostatin (Pola Pharma, Tokyo, Japan) treatment. For induction of DNA replication stress, MEFs were treated with hydroxyurea (HU).

Antibodies, immunostaining and Western blotting

Antibodies against γH2AX (JBW301, Upstate Biotechnology) and H2AX (Bethyl) were used for immunostaining and Western blot analysis. Antibodies against β-actin (AC-74, Sigma), PCNA (Santa Cruz) and histone H3 (ab1791, Abcam) were used for Western blot analysis. Prior to immunostaining with primary and secondary antibodies, cells were fixed with 4% paraformaldehyde for 10 min and permeabilized with 0.1% Triton X-100/PBS for 10 min. Western blot analysis and confocal microscopy were performed as described previously [10].

Transcription level analyses with RT-PCR

Total RNA was extracted from MEFs with the RNeasy system (Sigma). RNA (0.8 μg) was reverse-transcribed using a cDNA Archive kit (Applied Biosystems) and subjected to PCR. The following PCR primers were used: H2axf, 5′-TTGCTTC-AGCTTGGTGCTTAG-3′; H2axr, AACTGGTATGAGGC-CAGCAAC; β-actinf, CATCCAGGCTGTGCTGTCCCTGTA-TGC; and β-actinr, GATCTTCATGGTGCTAGGAGCCA-GAGC; Trp53-F, CGGATAGTATTTCACCCTCAAGATC-CG; Trp53-R, AGCCCTGCTGTCTCCAGACTC; Sidt2-F, CGGAAGGCTGGTTTCTGAGTTTCCG; Sidt2-R, CTGTA-AACGCCAAGGACCAGAA; Phlda3-F, CGGTCCATCTAC-